Precipitation of Microparticulate Organic Pigment Powders by a Supercritical Antisolvent Process

Lei Hong,* JiZhi Guo, Yong Gao, and Wei-Kang Yuan

UNILAB Research Center of Chemical Reaction Engineering, East China University of Science and Technology, 200237 Shanghai, People's Republic of China

The supercritical antisolvent (SAS) process has been used to produce submicronic Bronze Red particles. Among the process parameters, the pressure, temperature, and flow rate of the solution were studied. Two different solvents, ethanol and acetone, were also studied. The concentration of the liquid solution was kept unchanged in all of the experiments. The size and morphology of particles were affected by the temperature, pressure, and flow rate when ethanol was used as the solvent. Nevertheless, the size and morphology of the crystals precipitated from acetone were little sensitive to temperature and pressure but were influenced only by the flow rate. It was indicated that the interaction between the solute and the solvent played an important role in controlling the morphology and size of the crystals of Bronze Red under the same concentration.

Introduction

Organic pigments provide highly decorative and/or functional effects when applied as paints, inks, leather finishes, plastics, elastomers, paper goods, textiles, etc. The application properties and the final color value of pigmented systems are a function of the physical properties of the pigment (including the particle size distribution, morphology, and crystal configuration) and are dependent on the way the pigment is made. For instance, to ensure a maximum color value, the pigment should be in the optimum size range according to the Mie theory (the color strength is a function of the particle size, refractive index n, and absorption coefficient k). Besides color strength, other properties such as transparency, opacity, and flow are known to be a function of the pigment particle size.

Pigment manufacturers are devoting considerable effort toward finding the best way to make their products with optimal physical properties. This includes the investigation of postconditioning or after-treatments to reach this objective.[1] Generally, there are two after-treatment methods in industrial production: recrystallization from organic solution and machinery comminution (crushing, grinding, milling, etc.). However, these two methods suffer from some drawbacks such as a wide particle size distribution and an environmental pollution problem associated with the use of an organic solvent for the solution of organic pigment,[2,3] etc.

Therefore, it is desirable to explore alternative methods, which at least partially resolve those problems. Supercritical antisolvent (SAS) recrystallization has been considered as a promising new technique to produce solvent-free microparticles with a narrow size distribution. The solvent can be removed completely by the SAS, leaving a dry precipitate. The mixture of solvent and antisolvent can be separated when it is depressurized. Then the liquid solvent and gaseous antisolvent can be recycled. Hence, the SAS process provides a potential to resolve the environmental problem in the after-treatments of organic pigments. Moreover, modulating the rate at which the liquid and supercritical phases are brought into contact allows for control of the rate of precipitation. In turn, this affects the size and morphology of particles.

In recent years, supercritical fluids are used as an antisolvent, and this process has been proven to be very effective in certain fields.[4] Generally, there are two methods of applying the SAS technique. The first is a semibatch mode, which is known as the gas antisolvent (GAS) process.[5−8] In this mode, the supercritical fluid is introduced into an already existing and stationary bulk liquid phase. The second technique is a continuous operation, in which a spray of liquid solution is fed through a capillary nozzle as fine droplets into a vessel containing the supercritical fluid.[9] The continuous SAS process shares many similarities with classical spray-drying techniques. The major difference lies in spraying the solution into a supercritical fluid instead of into the heated air as the external phase. The SAS is quite miscible with the organic solvent; however, it is a nonsolvent for the solute. The second method is also called precipitation with compressed antisolvents (PCA)[10−12] or an aerosol spray extraction system (ASES).[13] The most widely used SAS is CO_2, which offers various advantages. CO_2 has favorable critical properties. Furthermore, it is nontoxic, nonflammable, inexpensive, recyclable, and "generally regarded as environmentally acceptable". The properties of CO_2 can be adjusted by regulating the temperature and pressure of the system.

Generally, in the GAS process, the organic solvent cannot be completely removed, and additional processing treatments are needed before the dry product can be recovered. Thus, in our study, continuous SAS was introduced. It has been successfully studied in many fields. Dixon et al.[10] sprayed the polystyrene in a toluene solution into CO_2 and obtained polystyrene microspheres with diameters from 0.1 to 20 μm. Yeo et al.[14] produced the spherical particles of insulin ranging between 1 and 4 μm by precipitating it from dimethyl sulfoxide (DMSO) in supercritical CO_2 with GAS and SAS processes. Reverchon et al.[15] obtained particles of various morphologies at different expansion levels when

* To whom correspondence should be addressed. Telephone: 86-21-64253326. Fax: 86-21-64253528. E-mail: honglei_unilab@sohu.com.

10.1021/ie000129h CCC: $19.00
Published on Web 12/04/2000

the DMSO solution of yttrium, samarium, and neodymium acetates were sprayed into supercritical CO_2. Several excellent reviews of GAS/SAS/PCA were presented by Reverchon,[4] Subra and Jestion,[16] and Subramaniam et al.[17] Although many investigations have been accomplished, the phenomenon of solute crystallization is very complex, and only limited knowledge is actually available on the continuous SAS process.

As an attempt to overcome the drawbacks in the existing industrial pigment postprocessing, the aim of the present research was to apply the continuous SAS to producing submicronic particles of Bronze Red (a commercial pigment). The influences of operating variables (pressure, temperature, and flow rate of the liquid solution) on the size and morphology of particles were studied. Two different solvents were also studied.

Theory

Mechanism of Crystallization. Any crystallization operation can be considered to comprise three basic steps: (1) achievement of the supersaturation; (2) nucleation (formation of crystal nuclei); (3) growth of the crystals. The attainment of the supersaturation state is essential for any crystallization operation, and the degree of supersaturation is the prime factor controlling the precipitation process. Crystals of small size and of narrow distribution are obtained when solutes are consumed mainly by nucleation. The rate of nucleation and the growth rate will increase with an increase of the supersaturation. However, the rate of nucleation increases more rapidly than the growth rate. Thus, high supersaturation is beneficial to the formation of smaller particles with a narrow particle size distribution.

As soon as stable nuclei have been formed, they begin to grow into crystals. According to Volmer's theory, the crystal growth follows a two-dimensional growth mechanism. The concept of this mechanism is that the crystal growth is a discontinuous process, taking place by adsorption, layer by layer, on the crystal surface. Atoms, ions, or molecules will link into the lattice in the positions where the attractive forces are the greatest.

High supersaturation will often cause the preferential growth of a crystal in one particular direction, leading to the formation of needlelike particles. One of the possibilities is that a screw dislocation is formed on the crystal face, which causes the continuous growth in this direction.[18]

The two-dimensional growth mechanism may be disrupted at high temperatures or by the presence of impurities, such as an adsorbed solvent on the crystal surface. In cases where the edge free energy is small, the size of the critical two-dimensional nuclei is reduced to only one growth unit because of the increase of supersaturation. In this situation, there is no barrier for two-dimensional nucleation and continuous growth will occur. The nonfaceted growth takes place as the crystallographic orientation is lost. This roughening of the crystal face is called "kinetic roughening".[19]

SAS Process. In the SAS process, the particles form in consecutive steps: formation of droplets and crystallization in the droplets. Dixon et al.[10] observed that the spray atomized extremely close to the capillary nozzle to form very small droplets. They used the Weber number (N_{We}) to describe the size of the droplets:

$$N_{We} = \rho_A V^2 D/\sigma \quad (1)$$

where ρ_A is the antisolvent density, V is the relative velocity, D is the drop diameter, and σ is the interfacial tension. A large Weber number indicates that the deforming forces are larger than the reforming surface forces, hence leading to drop breakup into smaller droplets. When the antisolvent density and the relative velocity increase, the value of the Weber number will increase. With the change of the interfacial tension, the Weber number will also change.

After small droplets form, they are contacted with an excess of supercritical fluid. Because the solvent and the SAS are fully miscible, rapid transfer of the antisolvent into the droplet and evaporation of the organic solvent out of the droplet cause the droplet to swell rapidly. Antisolvent diffusion decreases the solute solubility within the organic phase, whereas solvent evaporation increases the solute concentration. Therefore, high supersaturation can be achieved and then small crystals are obtained.

Experimental Section

Material. The pigment used here was supplied by Shanghai No. 5 Dyestuff Co. The molecular formula of Bronze Red is $C_{23}H_{17}O_2N_3$, with a molecular weight of 367.41. The molecular structure of Bronze Red is as follows:[20]

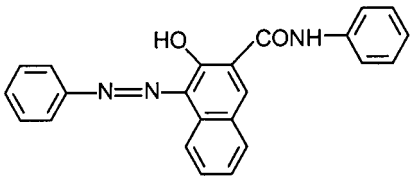

The untreated Bronze Red particles range from 1 to 5 μm (see Figure 1). The shapes of the particles are irregular. Carbon dioxide (as the antisolvent) was supplied by Shanghai Wujing Chemical Co. at 99.5% purity. Acetone (analytical reagent; Shanghai Feida Co., Ltd.) and ethanol (analytical reagent; Shanghai ZhengXing No.1 Chemical Co.) were used as the solvent. At 25 °C, the solubilities of Bronze Red are 2 and 1 mg of solute/mL of solvent in acetone and ethanol, respectively.

Apparatus. A schematic of the continuous SAS process is shown in Figure 2. The apparatus can be described as a continuous current precipitator in which the SAS and the liquid solution are separately fed at the top of the autoclave and concurrently discharged from the bottom. It consists of four sections: SAS (CO_2) supplying system; Bronze Red solution feeding unit; precipitator; gas−liquid separation section.

Two high-pressure pumps (Whitey Co., Highland Heights, OH) were used to deliver the Bronze Red solution and the supercritical CO_2, respectively. Before entering the pump, CO_2 was cooled to 0 °C using a cold trap to prevent it from cavitation. CO_2, in the line linking the pump and the precipitator, was heated by an electric coil (YD-3) controlled by a temperature controller (ÜGU AI-108 model).

A cylindrical vessel of 628 cm^3 internal volume (L = 50 cm and D = 4 cm) was used as the precipitator. The liquid solution was fed to the precipitation chamber

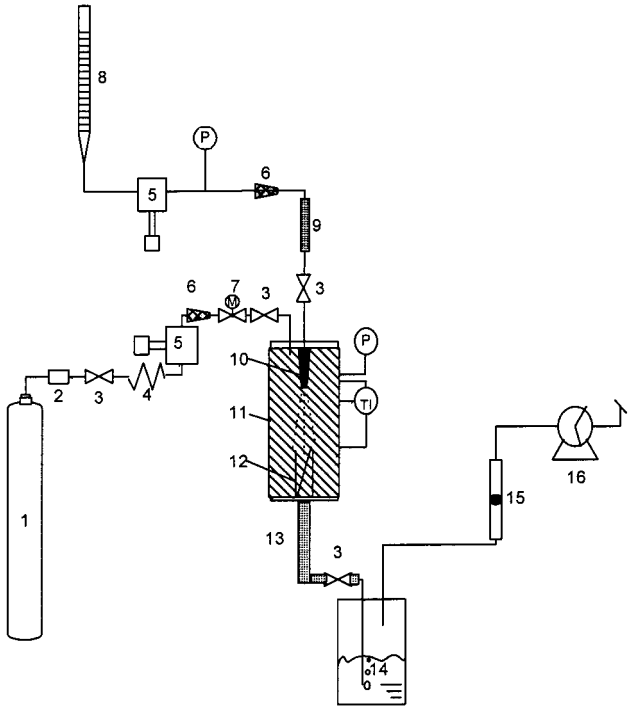

Figure 1. Schematic of the experimental apparatus for the continuous SAS process: (1) carbon dioxide cylinder; (2) purifier; (3) micrometering valve; (4) cool trap; (5) high-pressure pump; (6) check valve; (7) pressure-regulator valve; (8) liquid solution supply; (9) filter; (10) nozzle; (11) precipitator; (12) sampler; (13) coil heater; (14) separator; (15) rotameter; (16) wet testmeter.

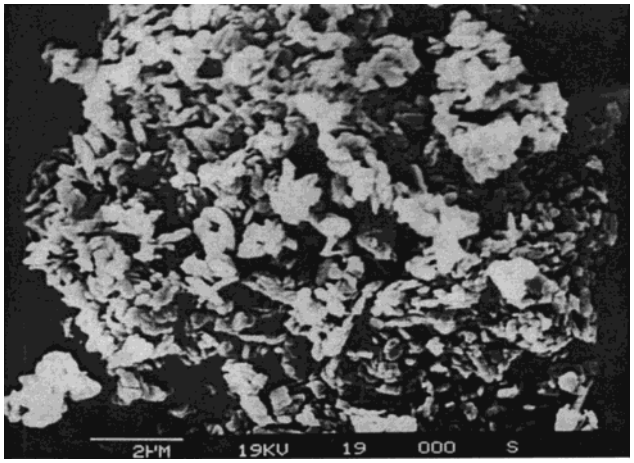

Figure 2. SEM photograph of the Bronze Red virgin material.

through a nozzle (50 μm diameter and 0.3 mm thickness). Supercritical CO_2 was fed through another inlet located at the top of the chamber. The precipitator was heated by electrical coils (1500 W) connected to a temperature controller (ÜGU A1-708 model), and a thermocouple was inserted in the chamber to measure the crystallization temperature. The pressure in the chamber was measured by a precision gauge (YB-150) and regulated by a micrometering valve (WL93H-320P) located at the exit of the vessel. To avoid clogging and to maintain a constant flow, this valve was heated by a coil heater (YD-3) connected to another temperature controller. The solid particles were collected on a glass slide placed at the bottom of the precipitator.

The miscible supercritical CO_2 and the organic solvent were discharged from the precipitator, splitting into two phases in the separator (a 10 L container). At the exit of the separator, a rotameter (LBZ-4) and a wet testmeter (BSD-0.5) were used to measure the CO_2 flow rate and the total quantity of antisolvent used.

Table 1. Experimental Conditions and Results (Ethanol as the Solvent)

run no.	T (K)	P (MPa)	flow rate (mL/min)	morphology	particle size (μm)
1	308	5.5	15	agglomerated rhombus	9−12
2	308	8.0	15	sphere	4−6
3	328	5.5	15	sphere	6−10
4	328	8.0	15	sphere	4−5
5	328	12.0	15	sphere	≈1
6	348	5.5	15	sphere	5−7
7	348	8.0	15	sphere	2−4
8	348	12.0	15	sphere	≈1
9	308	5.5	15	agglomerated rhombus	10−14
10	348	8.0	6	irregular sphere	6−8

Procedures. At the beginning of the continuous SAS process, CO_2 was fed to the precipitator until the desired pressure was reached. Then, a steady antisolvent flow was set. The flow rate was controlled at a designated value (ranging from 6.0 to 10.0 L/min). After the steady state was maintained for 15 min, the Bronze Red solution was pumped into the precipitator through the nozzle at a flow rate controlled according to the experimental planning. A 10 mL Bronze Red solution was then injected in each experiment. After injection, supercritical CO_2 continued to flow for 45−60 min to remove any residual organic solvent from the particles. If the final purge with pure CO_2 was not done, the organic solvent condensed during the depressurization and partly redisssolved the particles, modifying their morphologies. The fluid mixture (mainly CO_2 plus some organic solvent) left the precipitator for the separating tank.

Samples of the powder collected on the glass slide were observed by a scanning electronic microscope (SEM; Cambridge S250 MK3) and an optical microscope (Olympus BH-2).

Results and Discussion

During the spray process, the size and morphology of the Bronze Red particles are effected by many factors, such as the initial droplet size, mass-transfer rates between the solvent and antisolvent phases, nucleation kinetics, and crystal growth rates. To probe a possible mechanism which can control the particle size, we examined the effects of CO_2 pressure, temperature, and Bronze Red liquid solution flow rates as well as different solvents. Ethanol and acetone were used as the solvents, and the experiments were performed using the liquid solutions with the same concentration, 1 mg/mL.

Precipitation from an Ethanol Solution

Effect of Pressure and Temperature at a Constant Flow Rate. Table 1 shows the experimental conditions and the results in which ethanol is used as the solvent. To investigate the effect of antisolvent pressure on the particle morphology, we conducted several experiments, during which the temperature was held constant while the pressure was varied. As summarized in Table 1, the particle size significantly changes from 6−10 μm to about 1 μm, when the pressure is increased from 5.5 to 12.0 MPa at 328 K (runs 3−5). The same tendency is observed at 308 K (runs 1 and 2) and 348 K (runs 6−8).

When the solution is contacted with the SAS, ethanol presents a large volumetric expansivity, which increases

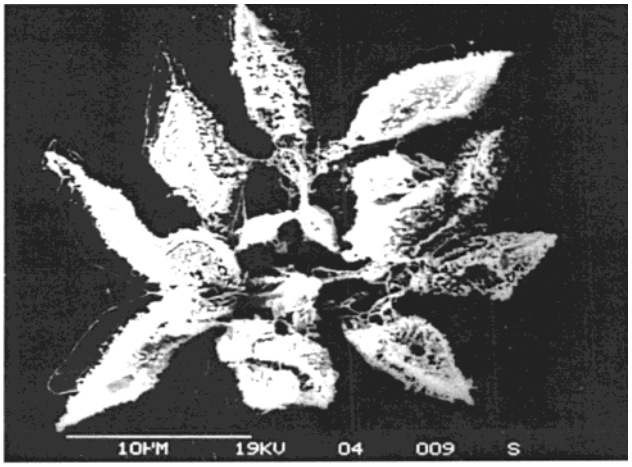

a

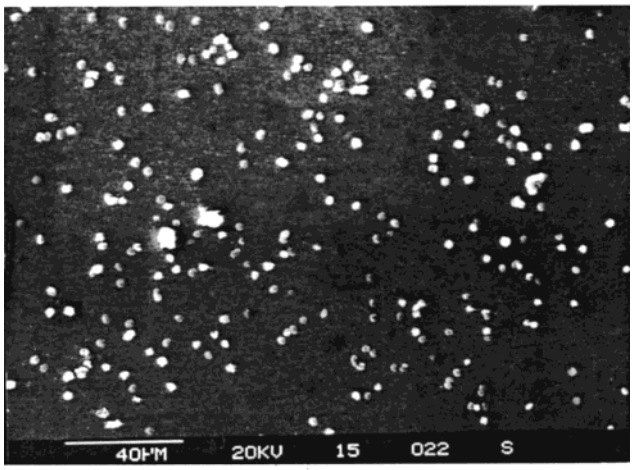

b

Figure 3. SEM photographs of Bronze Red particles precipitated from ethanol: (a) rhombic particles formed from run 1; (b) spherical particles formed from run 7.

remarkably with increasing pressure.[9,21] The expansivity causes the droplets to swell rapidly. More than one nucleation site might be present in each droplet. With an increase in the pressure, the expansivity also increases. More nucleation sites are formed in one droplet. Consequently, smaller particles are yielded with increasing pressure. This trend has also been observed by Reverchon et al.[15]

At higher temperatures, smaller particle sizes tend to be formed, as shown in Table 1. For instance, the particle size decreases from about 5 to 3 μm when the temperature increases from 308 to 348 K (see Figure 3b) at a pressure of 8.0 MPa (runs 2, 4, and 7).

Reverchon et al.[15] found that the size of yttrium acetate (AcY) particles produced by SAS showed a slight increment of the mean particle size with an increase in the temperature. They suggested that larger particles might be produced by higher growth rates at high temperatures. An explanation of the opposite trend that we observed is that the increase of the vapor pressure of ethanol (from 0.0138 MPa at 308 K to 0.0887 MPa at 348 K), as shown in Table 3, would be expected to exhibit higher mass-transfer rates. Rapid evaporation results in a high degree of supersaturation and subsequently the smaller particles are expected to precipitate because of higher nucleation rates. Meanwhile, the diffusivities of CO_2 and ethanol become larger with an increase of the temperature. On the other hand, the solution concentration in our study (1 mg/mL) is lower than that used by Reverchon at el. (15 mg of solute/mL). Consequently, the crystals cannot grow further because there are fewer solute molecules which can be used in crystal growth after nucleation. The mean particle size, therefore, decreases with an increase in the temperature, though the crystal growth rate increases.

Table 2. Experimental Conditions and Results (Acetone as the Solvent)

run no.	T (K)	P (MPa)	CO_2 density[24] (g/cm^3)	flow rate (mL/min)	morphology	particle size (μm)
11	308	8.0	0.4153	6	needle	10−15
12	308	8.0	0.4153	15	sphere	4−6
13	328	8.0	0.2121	6	needle	9−12
14	328	8.0	0.2121	15	sphere	3−5
15	328	12.0	0.4702	6	needle	10−12
16	328	12.0	0.4702	15	sphere	3−5
17	348	12.0	0.3297	15	sphere	3−4

Table 3. Vapor Pressure of Ethanol and Acetone[25]

	vapor pressure (MPa)			vapor pressure (MPa)	
T (K)	ethanol	acetone	T (K)	ethanol	acetone
308	0.0138	0.0463	348	0.0887	1.847
328	0.0376	0.969			

Moreover, it is noted that the rhombic particles with the size of 9−12 μm are obtained under 5.5 MPa and 308 K (see Figure 3a). Particles from run 9 show the approximate shape and size. In the gaseous CO_2 under 5.5 MPa and 308 K, ethanol does not completely evaporate before the droplets fall on the glass slide for SEM analysis. A liquid film is formed on the surface of the collector. It seems that the crystals grow up in the solvent film with less effect of the gaseous antisolvent, following the two-dimensional growth mechanism. Because of crystal anisotropy, the diamond particles with regular crystalline facets can be observed.

However, when the pressure and temperature increase, high supersaturation is achieved. At high supersaturation, nonfaceted growth occurs as the crystallographic orientation is lost. Consequently, kinetic roughening results in small spherical particles.

Influence of the Flow Rate. As described in eq 1, the flow rate is an important factor to droplet breakup. The experiments at different solution flow rates (15 and 6 mL/min), 348 K, and 8.0 MPa are performed (runs 7 and 10). The sizes of the particles in runs 7 and 10 show an increase of the mean particle size with an increase of the flow rate. A high flow rate (i.e., high relative velocity) results in a high Weber number. Smaller initial droplets are formed, leading to the smaller particles.

Precipitation from Acetone. Although Yeo et al.[14] and Reverchon et al.[15] found that the particle size of the solute was insensitive to the chemical composition of the liquid carrier, we found that a difference of the solvents might cause change of the particle size and morphology. The same results were reported by Thiering et al.[22] and Schmitt et al.[23]

The experimental conditions and results of CO_2/acetone/Bronze Red are summarized in Table 2. The size and morphology of the crystals are sensitive to the temperature and pressure when ethanol is used as the solvent, but they are little sensitive to the change of the temperature and pressure when acetone is used as the solvent. A difference in the morphology was observed from runs 11 and 12 operated under the same temper-

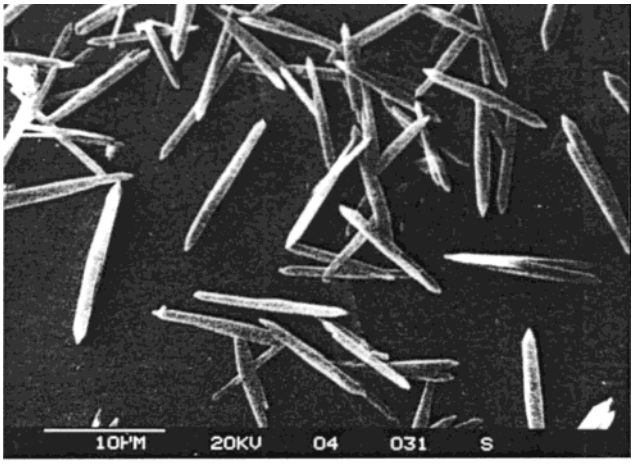

a

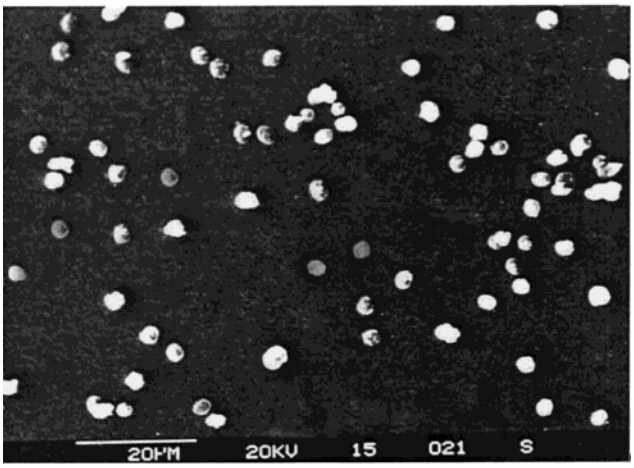

b

Figure 4. SEM photographs of Bronze Red particles precipitated from acetone: (a) rodlike particles formed from run 13; (b) spherical particles formed from run 14.

ature and pressure but a different flow rate. Similar results can be found in runs 13 (see Figure 4a), 14 (see Figure 4b), and 15 and 16. Besides, the particles precipitated from acetone are generally larger than those from ethanol under the same operation conditions.

The different results suggest that the mechanism of formation of particles from acetone is different from that from ethanol. The high vapor pressure of acetone (Table 3) might indicate that the rate of acetone evaporation from the droplets into the antisolvent is much more rapid than the rate of the antisolvent diffusion into/in the droplets under the experimental conditions. Consequently, swelling and breakup occurring in the CO_2/ethanol/Bronze Red system do not take place in the CO_2/acetone/Bronze Red system. A droplet forms a single microparticle.

Besides, ethanol has a larger affinity for the hydroxyl group of Bronze Red than acetone has, because of its high hydrogen-bonding potential. That ethanol strongly adsorbs onto the edge of a crystal lattice reduces the opportunity of solute molecules attaching to the surface of a crystal. Hence, this may lead to interruption of further growth of a crystal. On the contrary, the weaker attraction between acetone and Bronze Red leads to crystal growth without interruption.

So, the size of particles precipitated from acetone is determined by the initial droplet size and not by the temperature and pressure. Also, the particles crystallized from an ethanol solvent are generally smaller than those from acetone.

Furthermore, in runs 11, 13, and 15 that were operated at a lower flow rate of 6 mL/min, analogous needlelike crystals with a length of about 10 μm were observed. In addition, smaller spherical particles were observed in runs 12, 14, 16, and 17 when all of these experiments were operated at a higher flow rate of 15 mL/min. This indicates that the size and morphology of particles crystallized from an acetone solution are sensitive to the solution injection flow rate.

As discussed in the Theory section, the larger the Weber number, the smaller the droplets. In these experiments in which acetone was used as the solvent, the flow rate changed greatly and so did the relative velocity. [The velocities in the nozzle in this study ranged from 50 m/s (6 mL/min) to 127 m/s (15 mL/min).]. Also, the relative velocity term in the Weber number is squared, and thus it has a great influence on the Weber number. The value of the antisolvent density, ranging from 0.2121 to 0.4702 g/cm^3 that we studied, is small compared to the value of the velocity. Therefore, the contribution of the antisolvent density to the value of N_{We} is smaller. Besides, Bronze Red is not a surfactant, and its concentration in acetone is low. Thus, the change of the interfacial tension of the solution under the experimental conditions is small. As a result, the initial droplet size is primarily determined by the flow rate of the solution.

At the low flow rate, 6 mL/min, bigger initial droplets were obtained. Because of the formation of the screw dislocation on one of the crystal faces at high supersaturation, the needlelike particles are precipitated. However, when the relative velocity was higher, 15 mL/min, the smaller initial droplets were formed. There are a few molecules which can be used in the growth of the crystal and the screw dislocation in the small droplets. So, small spherical particles are obtained.

Conclusion

Precipitation of Bronze Red microparticles can be made through the continuous SAS process. The size and morphology of Bronze Red particles could be manipulated by variation of the system temperature and pressure, the flow rate of the solution, and the solvent used. The nature of the solute and solvent interaction plays an important role in the formation of the particles of Bronze Red. The strong interaction always leads to large particles. The size and morphology of particles precipitated from ethanol are influenced by the temperature, pressure, and flow rate. However, the flow rate of the solution basically affects the size and morphology of particles precipitated from the acetone solution.

More generally, favorable flexibility of preparing microparticles of different sizes and morphologies and the potential of conquering the environment problems discussed above render the supercritical-based process more competitive than the conventional postprocessing treatments of organic pigment.

Acknowledgment

The authors gratefully acknowledge the financial support of the Shanghai Natural Science Foundation from Shanghai Science and Technology Committee. The

authors also thank Professor Hong-Lai Liu and Professor Si-Yong Zhuang for their assistance.

Literature Cited

(1) Patton, T. C. *Pigment Handbook (Volume III): Characterization and Physical Relationships*; John Wiley & Sons: New York, 1973.

(2) Mo, S. C. *Organic Pigment* (Chinese); Chemical Industrial Press: Beijing, 1988.

(3) Zhuang P. Dispersion of Organic Pigment. *Dyest. Ind. (Chinese)* **1994**, *2*, 4.

(4) Reverchon, E. Supercritical Antisolvent Precipitation: its Application to Micro-particle Generation and Products Fractionation. *Proceedings of the 5th Meeting on Supercritical Fluids*: *Materials and Natural Products Processing*, Institut National Polytechnique de Lorraine: Nice, France, 1998; Perrut, M., Subra, P., Chairmen; ISBN 2-905-267-28-3, Vol. 1, p 221.

(5) Gallagher, P. M.; Coffey, M. P.; Krukonis, V. J.; Klasutis, N. Gas Antisolvent Recrystallization: New Process to Recrystallize Compounds Insoluble in Supercritical Fluids. *Supercritical Fluid Science and Technology*; Johnston, K. P., Penninger, J. M. L., Eds.; ACS Symposium Series 406; American Chemical Society: Washington, DC, 1989; p 334.

(6) Berends, E. M. *Supercritical Crystallization: the RESS Process and the GAS Process*. Ph.D. Thesis, Delft University of Technology, Delft, The Netherlands, 1994.

(7) Berends, E. M.; Bruinsma, O. S. L.; de Graauw, J.; van Rosmalen, G. M. Crystallization of Phenanthrene From Toluene with Carbon Dioxide by the GAS Process. *AIChE J.* **1996**, *42*, 431.

(8) Dixon D. J.; Johnston, K. P. Molecular Thermodynamics of Solubilities in Gas Antisolvent Crystallization. *AIChE J.* **1991**, *37*, 1441.

(9) Reverchon, E.; Celano, C.; Porta, D. G. Supercritical Antisolvent Precipitation: A New Technique for Preparing Submicroic Yttrium Powders to Improve YBCO Superconductors. *J. Mater. Res.* **1998**, *13*, 284.

(10) Dixon, D. J.; Johnston, K. P.; Bodmeier, R. A. Polymeric Materials Formed by Precipitation with a Compressed Fluid Antisolvent. *AIChE J.* **1993**, *39*, 127.

(11) Bodmeier, R.; Wang, H.; Dixon, D. J.; Mawson, S.; Johnston, K. P. Polymeric Microspheres Prepared by Spraying into Compressed Carbon Dioxide. *Pharm. Res.* **1995**, *12*, 1211.

(12) Dixon, D. J.; Luna-Barcenas, G.; Johnston, K. P. Microcellular Microspheres and Microballoons by Precipitation With a Vapor−liquid Compressed Fluid Antisolvent. *Polymer* **1994**, *35*, 3998.

(13) Bleich, J.; Mueller, B. W. Production of Drug Loaded Microparticles by the Use of Supercritical Gases with the Aerosol Solvent Extraction System (ASES) Process. *J. Microencapsulation* **1996**, *13*, 131.

(14) Yeo, S. D.; Lim, G. B.; Debenedetti, P. G.; Bernstein, H. Formation of Microparticulate Protein Powders Using a Supercritical Fluid Antisolvent. *Biotechnol. Bioeng.* **1993**, *41*, 341.

(15) Reverchon, E.; Porta, G. D.; Trolio, A. D.; Pace, S. Supercritical Antisolvent Precipitation of Nanoparticles of Superconductor Precursors. *Ind. Eng. Chem. Res.* **1998**, *37*, 952.

(16) Subra, P.; Jestion, P. Powders Elaboration in Supercritical Media: Comparison with Conventional Routes. *Powder Technol.* **1999**, *103*, 2.

(17) Subramaniam, B.; Rajewski, R. A.; Snavely, K. Pharmaceutical Processing with Supercritical Carbon Dioxide. *J. Pharm. Sci.* **1997**, *86*, 885.

(18) Mullin, J. W. *Crystallisation*, 2nd ed.; Butterworth: London, 1972.

(19) Jetten, L. A. M. J.; Human, H. J.; Bennema, P.; van der Eerden, J. P. On the Observation of the Roughening Transition of Organic Crystals, Growing from Solution. *J. Cryst. Growth* **1984**, *68*, 503.

(20) Yang, X. W.; Luo, Y. Y.; Li, J. C.; He, Y. B. *Handbook of Chemical Products: Dyestuff and Organic Pigment (Chinese)*; Chemical Industrial Press: Beijing, 1999.

(21) Tom, J. W.; Lim, G. B.; Debenedetti, P. G.; Prud'homme, R. K. *Supercritical Fluid Engineering Science: Fundamentals and Applications*; ACS Symposium Series 514; American Chemical Society: Washington, DC, 1993; p 238.

(22) Thiering, R.; Charoenchaitrakool, M.; Sze, Tu L.; Dehghani, F.; Dillow, A. K.; Foster, N. R. Crystallization of Para-Hydroxybenzoic Acid by Solvent Expansion with Dense Carbon Dioxide. *Proceedings of the 5th Meeting on Supercritical Fluids: Materials and Natural Products Processing*, Institut National Polytechnique de Lorraine: Nice, France, 1998; Perrut, M., Subra, P., Chairmen; ISBN 2-905-267-28-3, Vol. 1, p 291.

(23) Schmitt, W. J.; Salada, M. C.; Shook, G. G.; Speaker, S. M., III. Finely-Divided Powders by Carrier Solution Injection into a Near or Supercritical Fluid. *AIChE J.* **1995**, *41*, 2476.

(24) Angus, S.; Armstrong, B.; DeReuck, K. M. *Carbon Dioxide: International Thermodynamic Tables of Fluid State—3*; Pergamon Press: Oxford, U.K., 1976.

(25) Shi, J.; Wang, J. D.; Yu, G. Z.; Chen, M. H. *Chemical Engineering Handbook (Chinese)*; Chemical Industrial Press: Beijing, 1996.

Received for review February 1, 2000
Revised manuscript received October 12, 2000
Accepted October 13, 2000

IE000129H